Proceedings of ERAD (2004): 45–50 © Copernicus GmbH 2004

ERAD 2004

Range-velocity ambiguity mitigation via phase coding: experimental results

J. C. Hubbert, S. Ellis, M. Dixon, and G. Meymaris

National Center for Atmospheric Research, Boulder CO, 80307 USA

Abstract. The Doppler Dilemma or range-velocity folding of echoes from uniformly spaced transmit pulse trains of weather radar poses a fundamental limit on radar data quality and is expressed by the following equation,

$$r_a v_a = c\lambda/8 \quad (1)$$

where r_a, v_a are the unambiguous range and velocity, respectively, for wavelength λ and where c is the speed of light. Since the product $r_a v_a$ is a constant for a particular wavelength, increasing either one (r_a,v_a) necessarily decreases the other. For $\lambda = 10$ cm (S-band) and a typical pulse repetition time (PRT) of 1 ms, $r_a = 150$ km and $v_a = 25\,m/s$. Weather phenomena routinely exceed both of these limits. Phase coding of the transmit pulses for single polarization radars (Sachidananda and Zrnić 1999) has been shown to be an effective method for the separation of range overlaid echoes thus extending r_a without compromising v_a. A systematic phase code is applied to the transmit pulses so that the simultaneous received echos from different trips (i.e., range overlaid echoes) will have distinct and separate phase codes. This allows for the separation of the estimates of the moments of the overlaid echoes up to about a 40 dB power ratio.

This paper discusses the SZ(8/64) phase coding algorithm and its implementation using SIGMET's RVP8 processor in S-Pol, NCAR's S-band radar. An important aspect of the algorithm is the censoring of data. The data quality of the radar moments that result from phase code processing are limited by power ratios, clutter power, spectrum width, SNR and spectra shapes. Censoring algorithms are discussed and experimental results are given.

1 Background

Detailed theory of SZ(8/64) phase coding can be found in Sachidananda and Zrnić (1999, henceforth referred to as SZ99). SZ99 have evaluated the technique using numerically simulated data while Frush et al. (2000) demonstrated the technique using experimental data from S-Pol, NCAR's S-band polarimetric radar. The technique was further statistically evaluated with experimental data in Hubbert et al. (2002) and Hubbert et al. (2003). Since the implementation of SZ phase coding is computationally intensive, the experimental evaluation of SZ the algorithm has been done by post processing data and not in real time; however, recent advances in radar processor technology have now made possible real time execution of phase coding algorithms. One such processor is SIGMET's RVP8 which NCAR has recently installed in parallel with the existing processor on S-Pol.

The systematic SZ(8/64) phase code is applied to the transmit pulses. When the first trip (considered the strong trip here) echoes are made coherent (i.e. by subtracting the applied phase code) the second trip becomes phase shifted by the SZ(8/64) *modulation code* (time series considered here are 64 in length). The spectrum of the phase modulated second trip echo consists of eight replicas of the spectrum of the unphase coded second trip echo. To recover the moments of the weak trip signal, at least two of these replicas need to be preserved. Thus, 3/4 of the weak trip spectrum may be "notched" or zeroed and this 3/4 notch is typically centered at the mean velocity of the coherent overlaid first trip. An attractive feature of the SZ phase code is that the auto covariance function of the phase code sequence is 1 for lags 0, 7, 15 etc. and zero otherwise. Thus, velocity estimates of the first trip coherent signal are unbiased by the overlaid modulated second trip echo. Overlaid echoes in effect behave as if they were white noise and do not bias the velocity estimates for the cohered trip.

The signal processing steps in executing the SZ(8/64) algorithm on unphase coded data are as follows: (moments with "ˆ" are recovered while others without "ˆ" are "truth" calculated from the original time series): 1) Phase code two time series, one as first trip the other as second trip and combine the sequences, 2) Create two sequences by cohering the combined sequence for the first and then second trip echoes,

Correspondence to: J. C. Hubbert
(hubbert@ucar.edu)

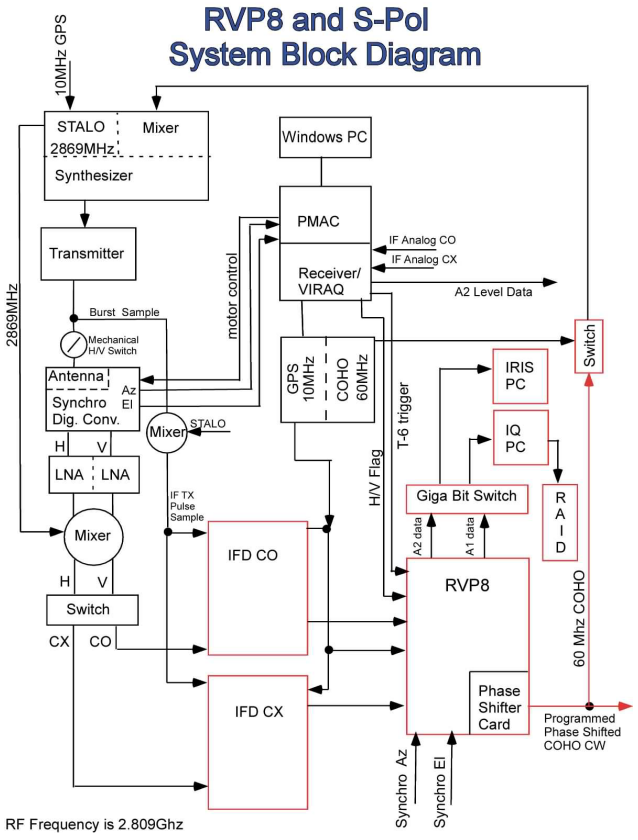

Fig. 1. Block diagram of the RVP8/S-Pol system. Newly added RVP8 system components are shown in red.

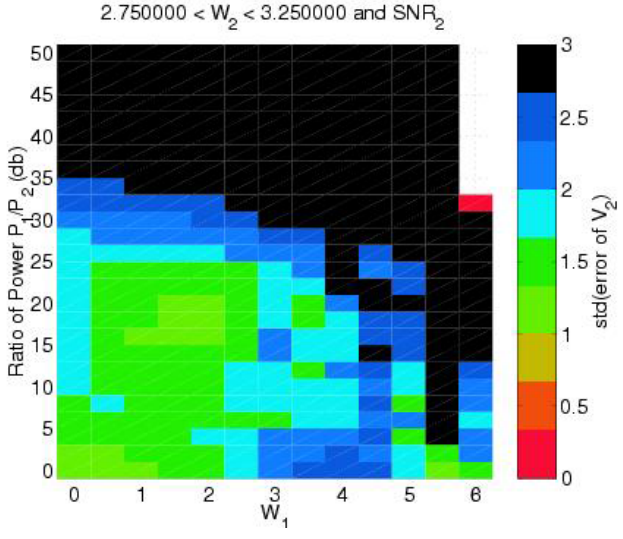

Fig. 2. The standard deviation of the errors of the recovered velocity $\hat{V}_2$ as a function of the power ratio P_1/P_2 and the width of the stronger trip signal, W_1.

3) Calculate $|R(1)|$ (first lag autocovariance) for both sequences; the greater one determines which trip is stronger; or the strong trip can be determined from a long PRT scan; 4) Calculate the power $\hat{P}_1$, velocity $\hat{V}_1$ and width $\hat{W}_1$ for the stronger trip (always referred to with the subscript "1" but not necessarily the first trip), 4) Apply a Hanning window to the combined time series and correct for the power loss, 5) Transform into the frequency domain via an FFT algorithm, 6) Apply 3/4 notch filter centered at the $\hat{V}_1$ estimated velocity, 7) Calculate the weaker trip power, $\hat{P}_2$, from the notched spectrum and multiply by 4 to account for the effects of the 3/4 notch, 8) If the recovered power ratio $P_1/P_2 < 20$ dB, $\hat{P}_1$ is corrected by subtracting $\hat{P}_2$, 9) Transform the notched spectrum back to the time domain (via an IFFT) and cohere to the weaker trip, 10) Calculate $\hat{V}_2$, and 11) Estimate the weaker trip spectrum width via the deconvolution method given in SZ99.

In May of 2003 the SIGMET RVP8 receiver/processor was installed in parallel to the existing S-Pol system. A simple block diagram of the S-Pol system is shown in Fig. 1. The blocks in red (or gray) are part of the newly installed RVP8 system. Both the integrated moments and the times series are output on a gigabit Ethernet connection to a gigabit switch that makes the data available to two workstation PCs called IRIS and IQ which further process and display the data. The time series data are stored on a terabyte RAID. The IQ PC is used to develop real time signal processing algorithms such as SZ(8/64) algorithm and subsequently the developed algorithm is programmed on to the RVP8. The SZ(8/64) algorithm has been developed in this way and now runs in real time on the RVP8.

Clutter filtering is an important aspect of data quality. Typically ground clutter power is removed via the use of IIR (infinite impulse response) filters which effectively remove the power around zero velocity but which also impart a phase delay which is non-linear. This phase delay will degrade the performance of the SZ algorithm causing unacceptable biases in $\hat{V}_2$, the weak trip velocity (Hubbert et al., 2003). To over come this, either spectral clutter filters or FIR clutter filters need to be used.

2 SZ Censoring

An important part of the SZ(8/64) algorithm is data censoring. There are two distinct types types of SZ algorithms and accompanying censoring algorithms: 1) SZ-1 and SZ-2. SZ-2 is used for lowest elevation angles (below about 1.5°) where long PRT scans are followed by phase coded short PRT scans. Information from the long PRT scan is used to censor the short PRT phase coded scan. The long PRT is about 3.1 ms (about 460 km unambiguous range) and the short PRT is about 788 μs (unambiguous range of 115 km and unambiguous velocity of about 32 m/s).

SZ-1 is used at higher elevation angles where the PRT can be adjusted so that only first and second trip echoes are possible. It is difficult for the SZ algorithm to separate more than two overlaid echoes. Since there is no accompanying long PRT scan, the SZ-1 recovered moments must be censored with the recovered data itself. Two techniques are discussed: 1) variance of the velocity field and 2) detection of excess

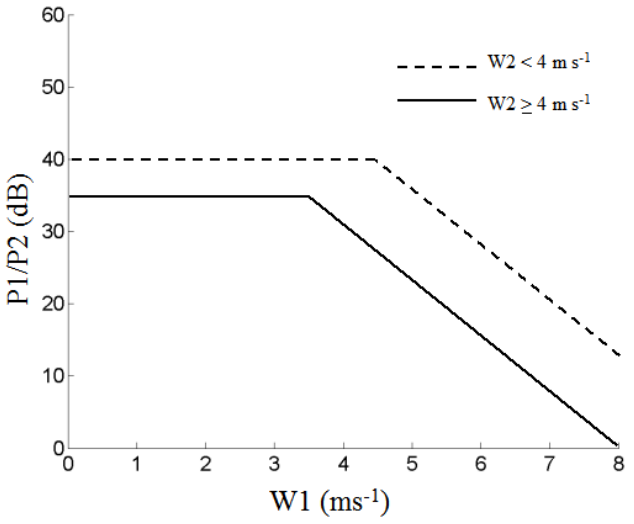

Fig. 3. SZ-2 censoring boundaries based on Fig. 2.

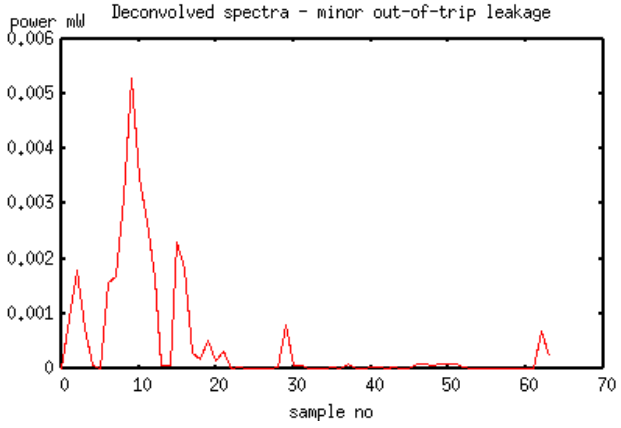

Fig. 4. An example of a good recovered weak trip spectrum.

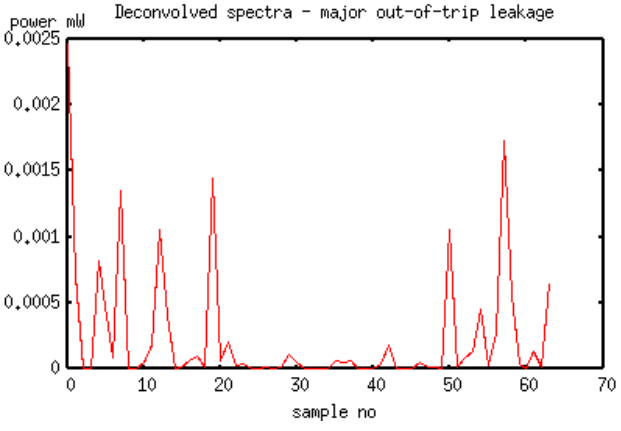

Fig. 5. An example of a bad recovered weak trip spectrum.

power in "spectral replicas" in the spectrum of the weak trip echo. Experimental data are given below to illustrate the censoring methods.

2.1 SZ-2 censoring

In the SZ-2 algorithm, powers are estimated from the long PRT data which is range unambiguous assuming maximum cloud tops of 18 km. The long PRT powers are used to sort the overlaid echoes of the short PRT scan. Short PRT data are used to estimate velocity and strong trip spectrum widths. Only moments from the strongest two trips are estimated, i.e., velocities from the third and fourth strongest trips are not estimated since it is difficult and recovery would be limited. Censoring of SZ-2 data is accomplished by four criteria: 1) SNR 2) SWR, signal to sum of weak trip powers ratio 3) P_1/P_2, the ratio of strong trip to weak power as a function of strong trip and weak trip widths and 4) SCR, the signal to clutter ratio. Criteria 1 simply requires that the received signal be above some power threshold based on the sensitivity of the radar. Criteria 2 uses the ratio of the in trip power to out of trip powers as calculated from the long PRT. For the strongest trip power P_1 and the second strongest trip power P_2, these criteria are

$$P_1/(P_2 + P_3 + P_4) \geq THRES1 \quad (2)$$

$$P_2/(P_3 + P_4) \geq THRES2 \quad (3)$$

The thresholds are typically set to $THRES1 = 0\,\text{dB}$, $THRES2 = 5\,\text{dB}$ in order to maintain acceptable variance of velocity estimates. Criteria 3 is based upon theoretical and experimental statistical plots such as shown in Fig. 2.

Figure 2 shows the standard deviation of the errors of the recovered weak trip velocity $\hat{V}_2$ as a function of the power ratio P_1/P_2 and the spectrum width of the stronger trip signal, W_1 with the spectrum width of W_2 restricted from $1.75\,\text{ms}^{-1}$ to $2.25\,\text{ms}^{-1}$ and for $v_a = 32\,\text{ms}^{-1}$. The time series data was gathered by the KOUN radar but was phase coded offline. If standard deviations of $2.5\,\text{ms}^{-1}$ are acceptable then $P_1/P_2 < 35\,\text{dB}$ for $W_1 < 2\,\text{ms}^{-1}$. As W_1 increases the recovery area shrinks. Based on such plots, censoring limits can be defined as shown in Fig. 3 which are simply straight lines.

2.2 SZ-1 censoring

For SZ-1 censoring, long PRT data is not available and the data must be censored based on the SZ recovered moments themselves. It was found that using the SZ-2 power ratio censoring technique for SZ-1 data was unacceptable due to the possible high standard deviations of the recovered moments. To overcome this, two new censoring techniques have been developed and tested: 1) a spectral quality estimate of the weak trip recovered spectrum which measures excessive power in the modulated spectrum replicas and 2) features of the texture of the velocity field. The spectral quality estimate of the recovered weak trip signal is based on the shape of the recovered spectrum after magnitude deconvolution. If the recovery was successful, the power will likely be concentrated around the center velocity estimate. An example of a good

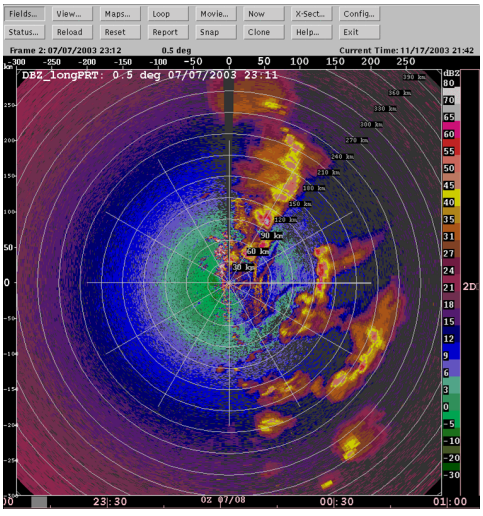

Fig. 6. Reflectivity from long PRT scan.

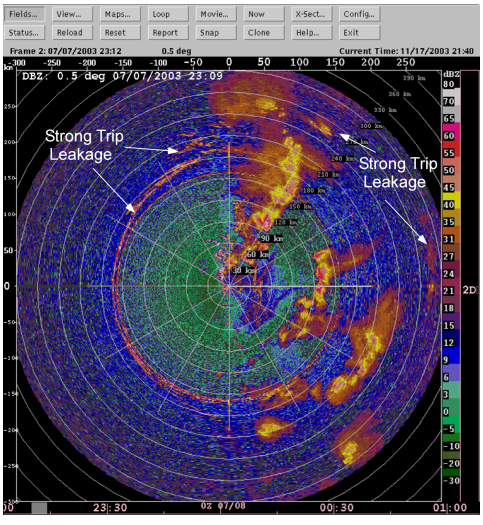

Fig. 7. SZ recovered reflectivity without censoring.

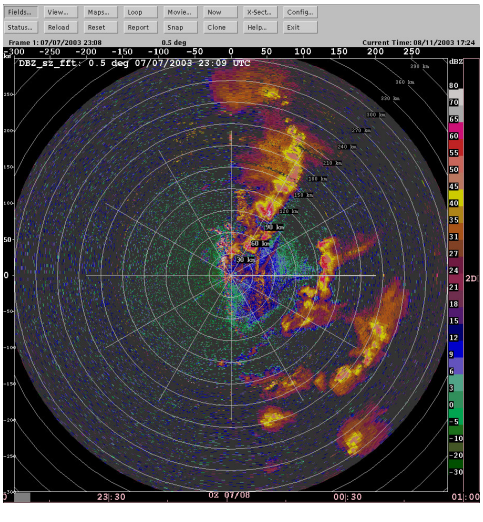

Fig. 8. Same as Fig. 7 but with SZ-1 censoring applied.

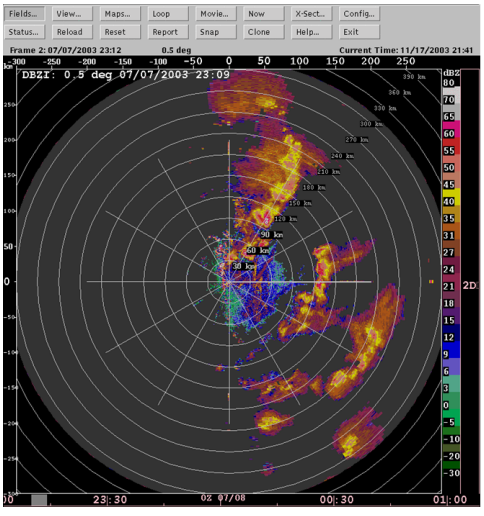

Fig. 9. Same as Fig. 8 but with additional signal processing to "clean up" the image.

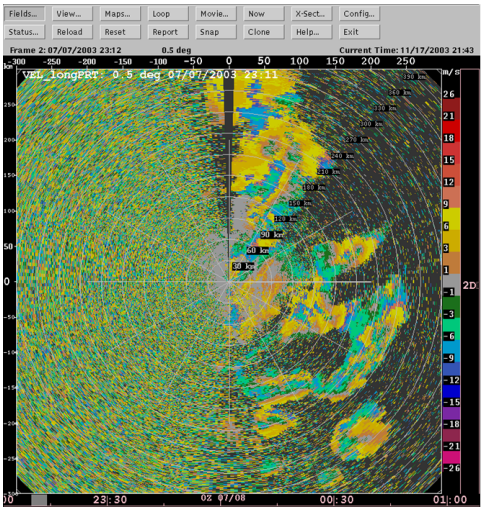

Fig. 10. Long PRT velocity corresponding to Fig. 6.

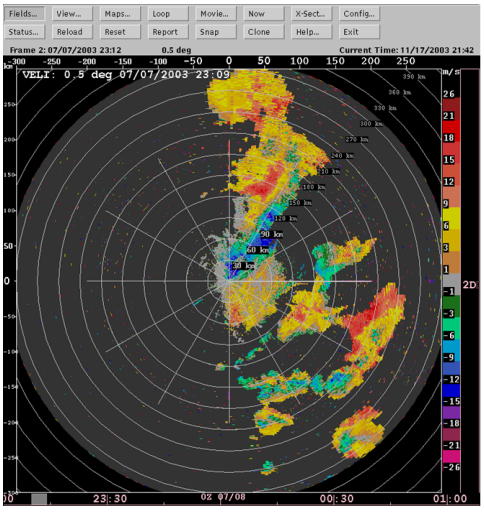

Fig. 11. SZ recovered velocity corresponding to Fig. 8.

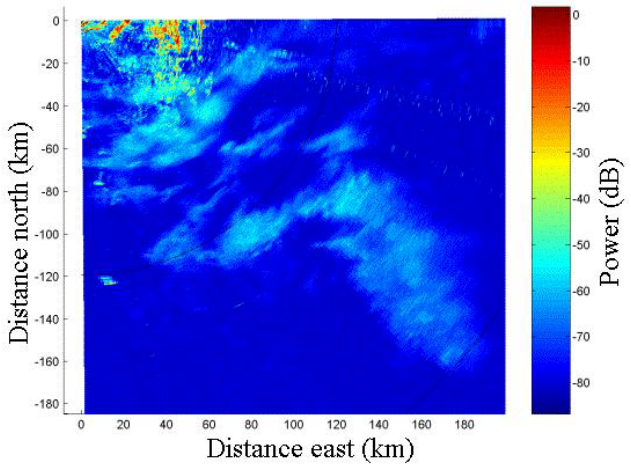

Fig. 12. SZ-2 long PRT power.

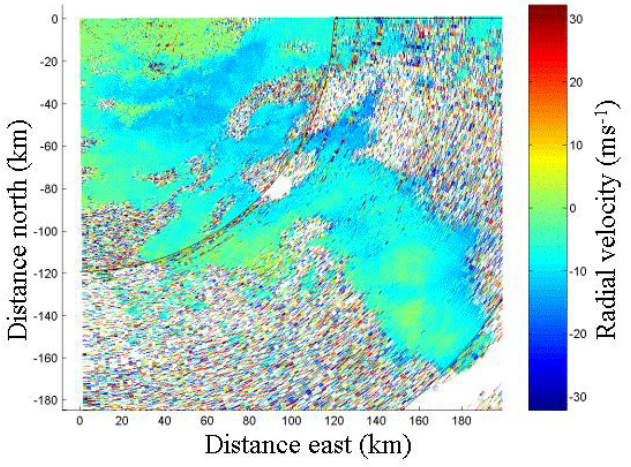

Fig. 13. SZ-2 recovered velocity.

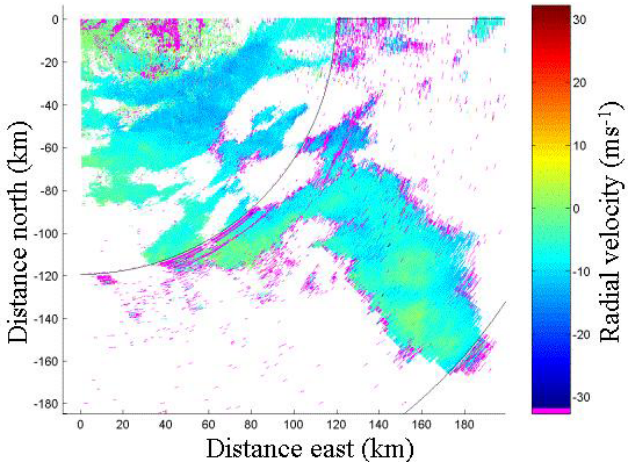

Fig. 14. SZ-2 censored recovered velocity.

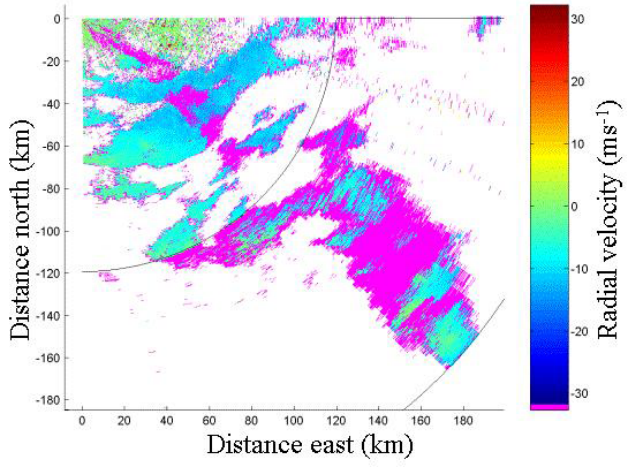

Fig. 15. WSR-88D recovered velocity.

recovered spectrum is shown in Fig. 4 while Fig. 5 shows a censored spectrum. The recovered weak trip spectrum is divided into eight segments based on the mean velocity estimate and the peak power in each segment is found. A ratio of the sum of the three weakest peak powers to the peak power is calculated and based on this ratio, a fuzzy logic membership function is created.

Poor SZ recovered velocity data quality is easily seen by the eye as high spatial velocity variance. Based on this observation, three estimates of the texture of the recovered velocity field are used for censoring: 1) a standard image texture estimator, 2) the radial spin of the velocity and 3) the azimuthal spin of the velocity. Spin is a measure of the number of inflections of a variable along a particular direction (Steiner and Smith 2000). The purpose of the spin estimates is to distinguish velocity fields that have high gradients due to meteorological convergence, divergence or circulation (e.g. tornadoes) from poor quality data. For example, a velocity field with a sharp gradient can have a high texture and thus be censored. However, the spin estimate would be low indicating that the velocity should not be censored. The three texture estimates and the spectral quality estimate are all inputs to a fuzzy logic algorithm that identifies the data to be censored.

3 Data Analysis

3.1 SZ-1 recovered data

The following data were gathered by S-Pol using RVP8 on 7 July 2003 at 0.7° elevation at the Marshall field site near Boulder, CO. A long PRT scan (PRT=2.7 ms) was followed by a short PRT (1.04 ms) phase coded scan about four minutes later. The unambiguous velocity and range for each scan are $v_a = 9.9\,\mathrm{ms}^{-1}$, $r_a = 405\,\mathrm{km}$ and $v_a = 25.7\,\mathrm{ms}^{-1}$, $r_a = 156\,\mathrm{km}$, respectively. The following plots compare the SZ recovered moments to the long PRT moments. Shown in Fig. 6 is the long PRT reflectivity and Fig. 7 shows the SZ recovered reflectivity with no censoring. By comparing the two plots, data quality problem areas are evident in Fig. 7. The ring of elevated reflectivity near 156 km range is caused by

first trip ground clutter leaking through to the first few gates of the second trip. Also shown in Fig. 7 are several other regions of strong trip power leakage. These areas should be censored. In Fig. 8, SZ-1 censoring has been applied and much of the previously indicated strong trip leakage areas indeed have been censored.

However, the censored image in Fig. 8 appears "rough" with data missing in some weather echo areas and with many speckles in echo free areas. The missing data areas can be infilled using interpolation from surrounding pixels but this should be done only in areas where the surrounding reflectivities are reasonably smooth and the data gaps are not too large. Many speckle filters exist (e.g., in the NEXRAD spec DV1208261F, this filter is referred to as the Strong Point Clutter filter, section 3.2.1.2.2) and they can be used to reduce speckles in the image. Figure 9 shows the reflectivity after infilling and speckle filtering and should be compared to the long PRT reflectivity in Fig. 6. There is excellent agreement especially in the high reflectivity areas. However, some of the lower reflectivity storm edges have been censored. There will always be a trade off between censoring of the low reflectivity areas and not censoring invalid data for a given set of thresholds. The thresholds chosen seem a reasonable compromise. Figures 10 and 11 are the long PRT velocity and the SZ recovered velocity, respectively. The SZ velocity agrees well with the long PRT velocity but has a much higher Nyquist velocity and therefore there is much less velocity folding.

3.2 SZ-2 recovered data

The following data was gathered by S-Pol at 0.5° elevation on 28 March 2004 using RVP8 at the Marshall field site near Boulder, CO. The long PRT is 3.125 ms and short PRT is 0.8 ms ($v_a = 32\,\mathrm{ms}^{-1}$). The long and short PRT scan are separated by about 30 s. Figure 12 shows the "power" (simply $I^2 + Q^2$ uncalibrated numbers) from the long PRT scan. The noise floor is at about -80 dB. The dark lines show the borders of the first and second trip echoes for the short PRT scan. Figure 13 shows the SZ-2 recovered velocity without censoring while Fig. 14 shows the SZ-2 recovered velocity with censoring. At 120 km in the beginning of the second trip in Fig. 13, leakage from the strong trip ground clutter causes the seen ring. The white areas of the censored image are due to the SNR threshold of 3 dB. The purple areas are due to statistical recovery boundaries of Fig. 3, the SWR ratios given above, or a SCR of -45 dB. Figure 15 shows the same velocity field of Fig. 14 but with the current NEXRAD WSR-88D censoring algorithm applied. The increase in the area of recovered velocity in Fig. 14 as compared to Fig. 15 is evident.

4 Summary

The SZ(8/64) algorithm has been programmed on SIGMET's RVP8 processor which is installed in S-Pol, NCAR's S-Band radar and is able to run in real time. The SZ algorithm makes possible the separation of overlaid echoes up to a 40 dB power ratio. At low elevations where more than two overlaid echoes are possible, a long PRT needs to accompany the short phase coded PRT (with a high unambiguous velocity) so that the location of the echoes are known unambiguously. The long PRT moments can also be used to censor the velocities calculated from the short PRT data. This is called the SZ-2 algorithm. At higher elevation angles where the short PRT scans only have two possible overlaid powers, the long PRT scan is not required. In this case the recovered moments are censored using the texture of the velocity field and a estimate of the quality of the weak trip recovered spectrum. A fuzzy logic routine is used to decide censoring. This is SZ-1 algorithm. Both algorithms were tested with experimental S-Pol data and evaluated with data from long PRT scans. The SZ-2 algorithm performance was compared to the current NEXRAD WSR-88D censoring algorithm and a dramatic increase in the amount of recoverable velocity estimates was demonstrated.

Acknowledgement. This research was supported by the ROC (Radar Operations Center) of Norman OK.

References

Frush, C., Doviak, R. J., Sachidananda, M., and Zrnić, D. S.: Application of the SZ Phase Code to Mitigate Range-Velocity Ambiguities in Weather Radars, JTECH, 19, 413–430, 2002.

Hubbert, J. C., Meymaris, G., and Keeler, R. J.: Range-Velocity Mitigation via SZ Phase Coding with Experimental S-Band Radar Data, 31st International Conf. on Radar Meteorology, pp. 727–729, 2003.

Hubbert, J. C. and Meymaris, G.: NEXRAD Range-Velocity Mitigation: Performance Evaluation of the SZ(8/64) Phase Coding Algorithm for Experimental Data, NCAR Annual Report to the Radar Operations Center, Norman OK, 2002.

Sachidananda, M. and Zrnić, D. S.: Systematic Phase Codes for Resolving Range overlaid Signals in a Doppler Weather Radar, J. Atmos. Oceanic Technol., 16, 1351–1363, 1999.

Steiner, M. and Smith, J. A.: Use of three-dimensional reflectivity structure for automated detection and removal of nonprecipitating echoes in radar data, J. Atmos. Oceanic Technol., 19:673–686, 2002.